Inorganic Chemistry

Article

pubs.acs.org/IC

Structural Modification on Copper(I)-pyridylpyrimidine Complexes for Modulation of Rotational Dynamics, Redox Properties, and Phototriggered Isomerization

Michihiro Nishikawa,[†] Yusuke Takara, Yohei Hattori, Kuniharu Nomoto, Tetsuro Kusamoto, Shoko Kume,*[,‡] and Hiroshi Nishihara*

Department of Chemistry, School of Science, The University of Tokyo, 7-3-1 Hongo, Bunkyo-ku, Tokyo 113-0033, Japan

Supporting Information

ABSTRACT: The redox properties of copper pyridylpyrimidine complexes, which undergo linkage isomerism based on pyrimidine ring rotation, were compared under different coordination environments. A newly synthesized compound, [Cu(Mepypm)(L_{Mes})]BF_4 (**1**·BF_4, Mepypm = 4-methyl-2-(2′-pyridyl)pyrimidine, L_{Mes} = 2,9-dimesityl-1,10-phenanthroline) was compared with previously reported complexes of [Cu(MepmMepy)(L_{Mes})]BF_4 (**2**·BF_4, MepmMepy = 4-methyl-2-(6′-methyl-2′-pyridyl)pyrimidine), Cu(Mepypm)(DPEphos)]BF_4 (**3**·BF_4, DPEphos = bis[2-(diphenylphosphino)phenyl]ether), [Cu(Mepypm)(L_{Anth})]BF_4 (**4**·BF_4, L_{Anth} = 2,9-bis(9-anthryl)-1,10-phenanthroline), and [Cu(Mepypm)(L_{Macro})]BF_4 (**5**·BF_4). Isomer ratios, isomerization dynamics, redox properties, and photoelectron conversion functions varied with the coordination structure. Methyl substituents on the 6-position of the pyridine moiety increased steric repulsion and contributed to quicker rotation, enhanced photoluminescence, and increased photodriven rotational isomerization.

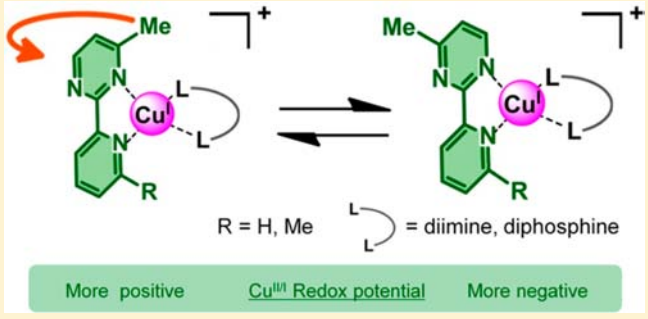

INTRODUCTION

Metal complexes bearing isomerizable ligands attract a great amount of interest, because their bistable states can be used as molecular switches and memories.[1−10] Copper complexes bearing π-conjugated bidentate chelating diimines show reversible redox activities and photochemical properties that follow well-established dependencies upon their coordination structures.[5,8,11−16]

With the aim of generating electric signals from a single molecule via stimulated structural rearrangements, we formed copper complexes using bidentate ligands that each contained a coordinated pyrimidine moiety. Rotational isomerization allowed the ligand to assume either of two possible coordination geometries at the Cu center,[17−19] with the rotation depending upon the kinetic lability of the Cu−N bonds.[13] Heteroleptic copper complexes were prepared by established routes that prevented the formation of homoleptic complexes through the use of a bulky auxiliary ligand.[15] The rotational interconversion between the two isomers in the copper(I) state is described in Figure 1, where the notation of inner (*i*-Cu^I) and outer (*o*-Cu^I) isomers indicates the orientation of the pyrimidine ring. Both *i*-Cu^I and *o*-Cu^I are comparably stable[17] because the copper(I) state prefers a tetrahedral form.[12] In contrast, the crowded geometry of one-electron oxidized *i*-Cu^I (*i*-Cu^{II}) is more easily destabilized by steric repulsion than one-electron oxidized *o*-Cu^I (*o*-Cu^{II}),[17] since Jahn−Teller effects cause the copper(II) state to favor a

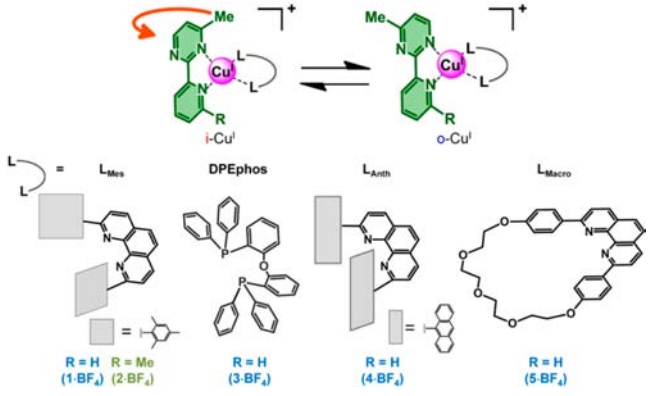

Figure 1. Schematic of the chemical equilibrium of the two rotational isomers, *i*-Cu^I and *o*-Cu^I, of newly synthesized **1**·BF_4, as well as that of previously reported compounds [Cu(MepmMepy)(L_{Mes})]BF_4 (**2**-BF_4, where MepmMepy = 4-methyl-2-(6′-methyl-2′-pyridyl)pyrimidine) and L_{Mes} = 2,9-dimesityl-1,10-phenanthroline),[18f] [Cu(Mepypm)(DPEphos)]BF_4 (**3**-BF_4, where DPEphos = bis[2-(diphenylphosphino)phenyl]ether),[18c,g] [Cu(Mepypm)(L_{Anth})]BF_4 (**4**-BF_4, where L_{Anth} = 2,9-bis(9-anthryl)-1,10-phenanthroline),[18a] and [Cu(Mepypm)(L_{Macro})]BF_4 (**5**·BF_4).[18a]

Received: May 7, 2013
Published: July 24, 2013

   dx.doi.org/10.1021/ic4011295 | *Inorg. Chem.* 2013, 52, 8962−8970

square planar geometry or a 5- or 6-coordinated form.[12] As a result, the redox potential of i-Cu^{II}/i-Cu^{I} (i-$Cu^{II/I}$) is more positive than that of o-Cu^{II}/o-Cu^{I} (o-$Cu^{II/I}$),[17] because i-Cu^{I} renders the oxidation of copper(I) to copper(II) thermodynamically less favorable.[12] We have previously demonstrated oxidation-triggered rotation (i-Cu^{I} − e^{-} → o-Cu^{II}) that is related to well-established copper(II/I) redox-triggered molecular machinery in a single molecule,[5] as well as the switching of electrode rest potential,[17,18a] intramolecular electron manipulation,[17,18b] and dual luminescence caused by pyrimidine ring rotational isomerization.[17,18c]

Our previous work has also demonstrated redox potential switching based on nonphotochromic photodriven rotation, i-Cu^{I} → o-Cu^{I}, and heat-driven rotation, o-Cu^{I} → i-Cu^{I}: [Cu(MepmMepy)(L_{Mes})]BF_4 (**2**·BF_4, where MepmMepy = 4-methyl-2-(6′-methyl-2′-pyridyl)pyrimidine) and L_{Mes} = 2,9-dimesityl-1,10-phenanthroline) demonstrated the switching at 203 K in the presence of a redox mediator, decamethylferrocenium ion ($DMFc^{+}$), via photoinduced electron transfer.[17,18f] In the present study, we synthesized a new variant of **2**·BF_4: [Cu(Mepypm)(L_{Mes})]BF_4 (**1**·BF_4, where Mepypm = 4-methyl-2-(2′-pyridyl)pyrimidine). H occupies the 6-position of the pyridine moiety in **1**·BF_4, compared with CH_3 in **2**·BF_4 (Figure 1).[17,18f] How this modification of the 6′-position of the pyridine moiety affects the rotational dynamics, photochemical properties, and photodriven rotation is also reported here. A comparison of [Cu(Mepypm)(L_{Mes})]BF_4 with previously reported complexes of [Cu(Mepypm)(DPEphos)]BF_4 (**3**·BF_4, DPEphos = bis[2-(diphenylphosphino)phenyl]ether),[18c] [Cu(Mepypm)(L_{Anth})]BF_4 (**4**·BF_4, L_{Anth} = 2,9-bis(9-anthryl)-1,10-phenanthroline),[18a] and [Cu(Mepypm)(L_{Macro})]BF_4 (**5**·BF_4)[18a] demonstrates the effects of the L_{Mes} moiety on ligand rotation and other properties of the complexes, because only the auxiliary ligand varies among them (Figure 1). Ligand rotation and the other properties of the complexes are shown to be strongly related to the coordination sphere, which is a finding that may aid rational molecular design for specific functionality.

RESULTS AND DISCUSSION

Synthesis, Characterization, Crystallography, and Rotational Dynamics of 1·BF_4. A new compound, **1**·BF_4, was synthesized via the reaction of tetrakis(acetonitrile)copper(I) tetrafluoroborate ([Cu(MeCN)$_4$]BF_4) with Mepypm and L_{Mes}[15] in dichloromethane at room temperature, according to a slight modification of our previously described method (Scheme 1).[18f]

X-ray structural analysis of **1**·BF_4·1.18CH_2Cl_2 reveals that both i-Cu^{I} and o-Cu^{I} forms were present in the same crystal (see Figure 2a and Table S1 in the Supporting Information). In a copper(I) complex the isotropic d^{10} electronic structure tends

Scheme 1. Synthesis of 1·BF_4

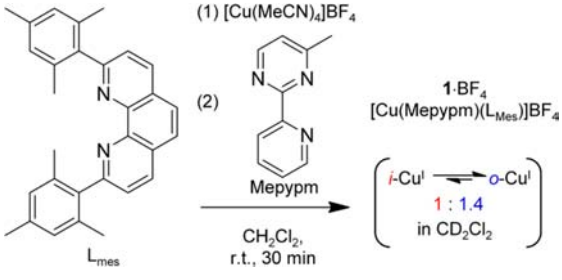

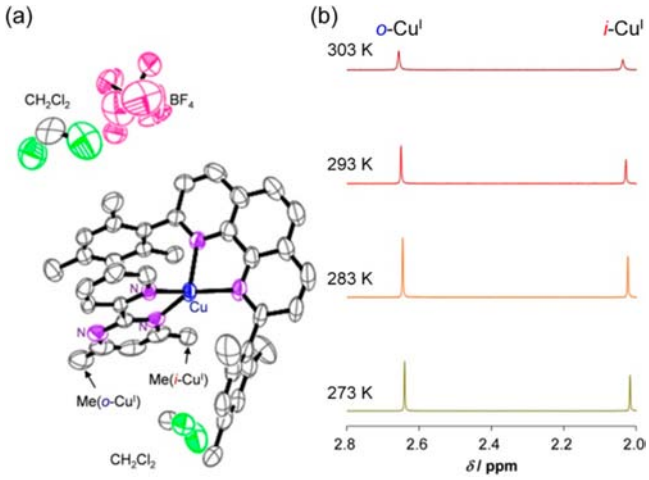

Figure 2. (a) ORTEP view of **1**·BF_4·1.18CH_2Cl_2. The displacement ellipsoids are drawn at a 50% probability level. Hydrogen atoms are omitted for clarity. (b) Temperature dependence of the methyl signal on the pyrimidine moiety in the ^{1}H NMR spectrum in CD_2Cl_2 in darkness.

to assume a distorted tetrahedral coordination geometry to minimize the ligands' mutual repulsion. The complex cation and the counterion were present in a 1:1 ratio in the asymmetric unit, suggesting an oxidation state of copper(I) in the single crystal. The crystal structure showed a disorder related to the methyl group on the pyrimidine moiety. This disorder indicated the coexistence of the i- and o-forms, because the only difference between the isomeric structures was the position of the methyl group. Occupancy refinement of the disorder gave a i-Cu^{I}:o-Cu^{I} isomer ratio of 46:54.

The rotational bistability of **1**·BF_4 in solution was confirmed by a previously described method[18] involving a nuclear magnetic resonance (NMR) spectroscopic study of the thermodynamics and kinetics of the molecular system's chemical equilibrium.[20] The ^{1}H NMR spectrum of **1**·BF_4 recorded in dichloromethane-d_2 (CD_2Cl_2) at 293 K shows two clearly resolved sets of signals, which were assigned to the i-Cu^{I} and o-Cu^{I} isomers (see Figure 2b and Figure S1 in the Supporting Information). The methyl substituents on the pyrimidine moiety in the o-Cu^{I} isomer showed signals (δ = 2.65 ppm) at positions similar to those shown by the uncoordinated ligand (δ = 2.61 ppm) in CD_2Cl_2. The corresponding signals shown by the i-Cu^{I} isomer were shifted upfield (δ = 2.03 ppm), because of the shielding at the Cu center and the aromatic moieties in L_{Mes}. The sharpness of signals indicates that the rotation was slower than the time scale of the ^{1}H NMR measurements. The molar ratio of the isomers in **1**·BF_4 (i-Cu^{I}:o-Cu^{I} = 1:1.4 at 293 K) was estimated by signal integration. van't Hoff plots were constructed from integration of the ^{1}H NMR signals recorded at several temperatures (see Figure S2 in the Supporting Information). The plots allowed the estimation of the variation of i-Cu^{I}:o-Cu^{I} ratio with temperature and aided the analysis of the subsequently recorded cyclic voltammograms. The broadening of the ^{1}H NMR signals recorded at 303 K indicates that interconvertion by ring rotation between the i-Cu^{I} and o-Cu^{I} isomers was occurring within the time scale of the ^{1}H NMR measurement (Figure 2b).

Characterization of Intramolecular Rotation. We used a modification of a reported method[21] to confirm the intramolecular nature of the interconversion via the ^{1}H NMR

dx.doi.org/10.1021/ic4011295 | Inorg. Chem. 2013, 52, 8962−8970

analysis of a mixed solution of [Cu(Mepypm)(L_{Mes})]BF_4 (**1**·BF_4) and [Cu(Mepypm)(DPEphos)]BF_4 (**3**·BF_4),[18c,g] which only differ in their auxiliary ligands.

The ^{1}H NMR spectrum of **1**·BF_4 recorded in acetone-d_6 at room temperature shows two sets of relatively sharp signals: one from *i*-Cu^I and one from *o*-Cu^I (Figure 3, top). Under

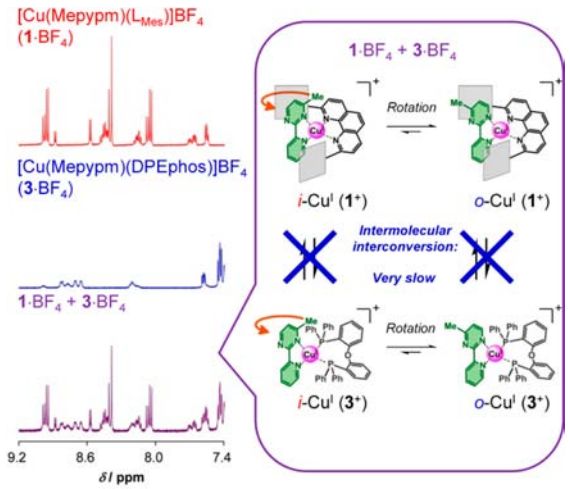

Figure 3. (left) Partial ^{1}H NMR spectra of **1**·BF_4 (top), **3**·BF_4 (middle), and a mixture of **1**·BF_4 and **3**·BF_4 (bottom) in acetone-d_6 in darkness at room temperature. (right) Illustration of the interconversion between species in a mixed solution of **1**·BF_4 and **3**·BF_4.

similar conditions, the two rotational isomers of **3**·BF_4 showed broadened ^{1}H NMR signals (Figure 3, middle) and the ^{1}H NMR spectrum of a mixed solution of **1**·BF_4 and **3**·BF_4 appears as a simple superposition of the spectra of the two individual components (Figure 3, bottom). This suggests that intermolecular interconversion between **1**·BF_4 and **3**·BF_4 was slow, compared with the time scale of the ^{1}H NMR measurement (Figure 3, right). Therefore, the interconversion between the *i*-Cu^I and *o*-Cu^I isomers of each **3**·BF_4 and **1**·BF_4 is dominated by intramolecular processes. The lack of signal fusion between **1**$^+$ and **3**$^+$ in the mixed solution precludes the possibility of faster intermolecular processes.

Electrochemistry of 1·BF_4. The rotational dynamics and electrochemical properties of **1**·BF_4 were studied via methods similar to those described in our previous study of **2**·BF_4.[18f] Fits were simulated for experimental cyclic voltammograms based on a square scheme between four stable isomers: *i*-Cu^I, *o*-Cu^I, *i*-Cu^{II}, and *o*-Cu^{II}. The shape of the voltammogram is strongly related to both the scan rate of the potential sweep and the nature of the rotational dynamics (Figure 4a).[22] Oxidation-triggered rotation, *i*-Cu^I − e$^-$ → *o*-Cu^{II} (Figure 4b), which is related to the well-established copper(II/I) redox-triggered rotation based on interlocked catenanes,[10g] is different from the desired phenomenon of photodriven rotation, *i*-Cu^I → *o*-Cu^I (Figure 1).

A voltammogram of **1**·BF_4 recorded at 275 K in Bu_4NBF_4−CH_2Cl_2 at a scan rate of 250 mV s^{-1} showed two reversible waves derived from the *o*-Cu$^{II/I}$ and *i*-Cu$^{II/I}$ redox reactions at $E^{\circ\prime}$ = 0.40 and 0.60 V vs Ag$^+$/Ag, respectively (see Figure 5a) ($E^{\circ\prime}$ = 0.78 and 0.98 V vs DMFc$^{+/0}$). *i*-Cu$^{II/I}$ showed a more positive $E^{\circ\prime}$ than *o*-Cu$^{II/I}$, because the bulky substituent around the copper prevented the assumption of the square planar geometry that is favored in the copper(II) state.[11,12] The

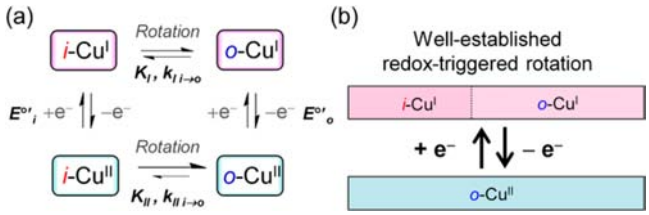

Figure 4. (a) Square scheme for simulation analysis comprising the redox reaction (vertical) and the pyrimidine ring rotation (horizontal). (b) The change of isomer ratio based on well-established redox-triggered rotation (*i*-Cu^I − e$^-$ → *o*-Cu^{II}), which is a different process from photodriven rotation (*i*-Cu^I → *o*-Cu^I).

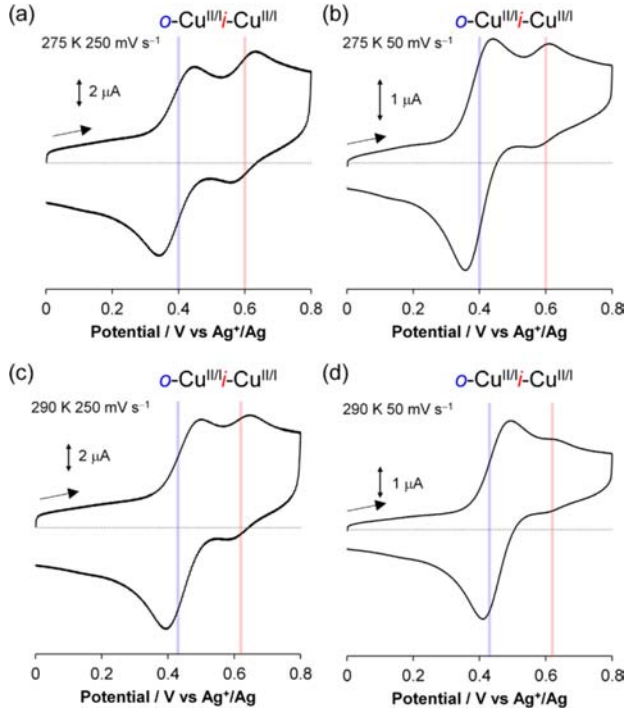

Figure 5. Cyclic voltammograms of **1**·BF_4 (0.5 mM) in 0.1 M Bu_4NBF_4−CH_2Cl_2: (a) at 275 K and a scan rate of 250 mV s^{-1}, (b) at 275 K and a scan rate of 50 mV s^{-1}, (c) at 290 K and a scan rate of 250 mV s^{-1}, and (d) at 290 K and a scan rate of 50 mV s^{-1}.

currents of the waves at $E^{\circ\prime}$ = 0.40 and 0.60 V were consistent with the *i*-Cu^I:*o*-Cu^I molar ratios estimated from the ^{1}H NMR measurements. As the scan rate of the potential sweep decreased to 50 mV s^{-1}, the two redox waves converged to that of *o*-Cu$^{II/I}$, particularly the cathodic waves (Figure 5b). Similar convergence was also observed at 290 K at a scan rate of 250 mV s^{-1} (Figure 5c). At 290 K and a scan rate of 50 mV s^{-1}, the redox wave for *i*-Cu$^{II/I}$ showed only a small trace; the redox wave for *o*-Cu$^{II/I}$ dominates the voltammogram (Figure 5d). The convergence of the cathodic waves suggests that oxidation promotes the rotation from *i*-Cu^{II} to *o*-Cu^{II} on the time scale of the potential sweep.[22] The preference of the square planar geometry in the copper(II) state favored the thermally activated conversion of *i*-Cu^{II} into *o*-Cu^{II}, because of the steric repulsion of the methyl group. This trend was continuously observed in voltammograms recorded at 265, 270, 275, 280, 285, and 290 K at scan rates of 50, 100, and 250 mV s^{-1} (see Table 1, as well as Table S2 and Figure S3 in the Supporting Information).

Two anodic waves derived from *i*-Cu$^{II/I}$ and *o*-Cu$^{II/I}$—the relative sizes of which reflect the *i*-Cu^I:*o*-Cu^I isomer ratio of the

dx.doi.org/10.1021/ic4011295 | Inorg. Chem. 2013, 52, 8962−8970

Table 1. Selected Parameters Obtained from the Simulated Cyclic Voltammograms of 1·BF_4 at Scan Rates of 250, 100, and 50 mV s^{-1} in 0.1 M Bu_4NBF_4−CH_2Cl_2

	285 K	280 K	275 K	270 K
$E^{o\prime}{}_o$ (V)[a]	0.42	0.41	0.4	0.38
$E^{o\prime}{}_i$ (V)[b]	0.62	0.61	0.6	0.59
K_I[c]	1.39	1.37	1.35	1.33
K_{II}[d]	4×10^3	5×10^3	6×10^3	1×10^4
$k_{Ii\rightarrow o}$[e] (s^{-1})	1	0.5	0.3	0.2
$k_{Io\rightarrow i}$[f] (s^{-1})	0.77	0.38	0.23	0.15
$k_{IIi\rightarrow o}$[g] (s^{-1})	1	1	0.5	0.5
$k_{IIo\rightarrow i}$[h] (s^{-1})	2×10^{-4}	2×10^{-4}	8×10^{-5}	5×10^{-5}

[a]Redox potential for *o*-$Cu^{II/I}$, vs Ag^+/Ag. [b]Redox potential for *i*-$Cu^{II/I}$, vs Ag^+/Ag. [c]Equilibrium constant, set as [*o*-Cu^I]/[*i*-Cu^I]. [d]Equilibrium constant, set as [*o*-Cu^{II}]/[*i*-Cu^{II}]. [e-h] [e]Rate constant for the *i*-Cu^I → *o*-Cu^I rotation. [f]Rate constant for the *o*-Cu^I → *i*-Cu^I rotation. [g]Rate constant for the *i*-Cu^{II} → *o*-Cu^{II} rotation. [h]Rate constant for the *o*-Cu^{II} → *i*-Cu^{II} rotation.

solution—were observed below 225 K (see Figure S4 in the Supporting Information). The cathodic wave for the *o*-$Cu^{II/I}$ of 1·BF_4 appeared very broad below 225 K, likely because the electron transfer rate of the reduction of the transient copper(II) complexes competed with the scan rate of the potential sweep (Figure S4 in the Supporting Information).

Thermodynamics and Kinetics of the Rotation of 1·BF_4. The equilibrium constants for the rotation in the initial state (K_I = [*o*-Cu^I]/[*i*-Cu^I]) of 1·BF_4 ranged from 1.0 to 1.4 over the temperature range of 203−293 K (Figure 6a), indicating that *i*-Cu^I and *o*-Cu^I were comparably stable. In contrast, a much larger equilibrium constant in the oxidized state (K_{II} = [*o*-Cu^{II}]/[*i*-Cu^{II}]) was obtained from the electrochemical analysis, indicating that nearly all molecules were present as the *o*-isomer under equilibrium when the system was oxidized from the initial copper(I) state (Figure 6b).

The rate constant for the *i*-Cu^I → *o*-Cu^I rotation, estimated from Arrhenius plots ($k_{Ii\rightarrow o}$) (Figure 6c), was $<10^{-5}$ s^{-1} at 203 K, indicating that the rotational motion was substantially frozen. This state of frozen rotation is labeled the "OFF state" (Figure 6e). At 250 K, $k_{Ii\rightarrow o}$ increased to 10^{-2} s^{-1}, indicating an activation of rotation in the copper(I) state. This corresponding state of activated rotation is labeled the "ON state". The rate constant for the *o*-Cu^I → *i*-Cu^I rotation ($k_{Io\rightarrow i}$), which is equal to $K_I^{-1}k_{Ii\rightarrow o}$, was of the same order of magnitude as $k_{Ii\rightarrow o}$, considering the value of K_I. In contrast, the rate constant for the *i*-Cu^{II} → *o*-Cu^{II} rotation estimated from the Arrhenius plots ($k_{IIi\rightarrow o}$) was 10^{-3} s^{-1} at 203 K (see Figures 6d and 6f), while that for the *o*-Cu^{II} → *i*-Cu^{II} rotation ($k_{IIo\rightarrow i}$ = $K_{II}^{-1}k_{IIi\rightarrow o}$) was negligibly small, because of the large value of K_{II}.

Effects of Methyl Substitution on Redox Properties and Rotational Dynamics. The effects of the substitution of a methyl group into the 6-position of the pyridine moiety on the complex's rotational dynamics and electrochemical properties were examined through a comparison of the present complex ([Cu(Mepypm)(L_{Mes})]BF_4 (1·BF_4), data described above) and a previously studied complex with an addition methyl group ([Cu(MepmMepy)(L_{Mes})]BF_4 (2·BF_4), data reproduced from our previous work in Table 2).[18f] Methyl substitution affected the rotation and redox behaviors in several ways: the Cu−N bond was electronically strengthened by the induction effects of the electron-donating methyl group; steric

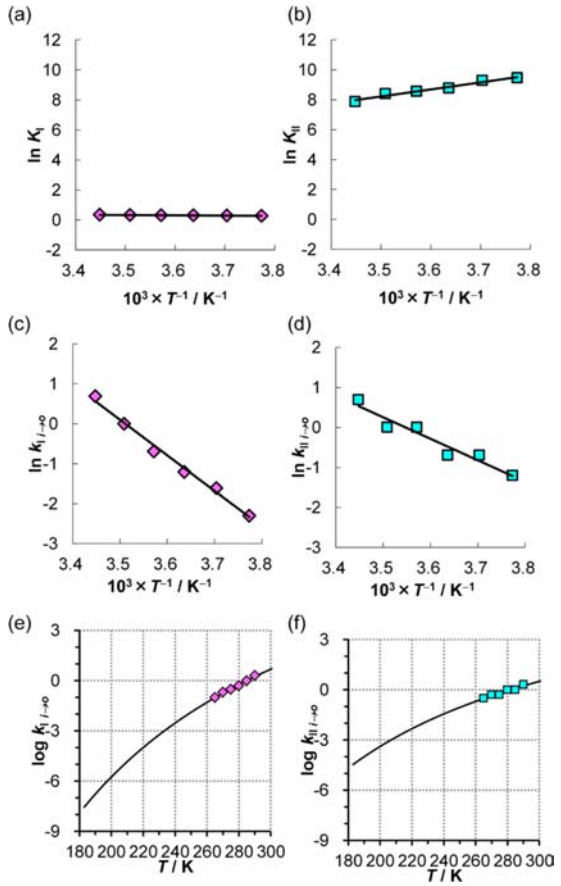

Figure 6. Thermodynamic and kinetic analysis of the rotational dynamics of the pyrimidine ring of 1·BF_4 in 0.1 M Bu_4NBF_4−CH_2Cl_2 in darkness: (a,b) van't Hoff plots, setting as K_I = [*o*-Cu^I]/[*i*-Cu^I] (a) and K_{II} = [*o*-Cu^{II}]/[*i*-Cu^{II}] (b); (c,d) Arrhenius plot for *i*-Cu^I → *o*-Cu^I (c) and *i*-Cu^{II} → *o*-Cu^{II} (d) rotational isomerization; (e,f) rate constants, $k_{Ii\rightarrow o}$ for *i*-Cu^I → *o*-Cu^I (e) and $k_{IIi\rightarrow o}$ for *i*-Cu^{II} → *o*-Cu^{II} (f), as a function of temperature, estimated from the Arrhenius plots. Values determined from simulated fits to the experimental cyclic voltammograms are shown as dots. Regression curves of the Arrhenius plots are indicated by lines.

repulsion between pyridylpyrimidine and the auxiliary ligand moieties was increased, because of the more-crowded coordination structures; and weak interactions, such as the CH_3−π interaction between the additional methyl group and mesityl moieties in the auxiliary ligand.

The two isomers, *i*-Cu^I and *o*-Cu^I, both coexisted in the solution; the *i*-Cu^I:*o*-Cu^I ratios in CD_2Cl_2 at 293 K were 1:1.4 for 1·BF_4 and 1:2.3 for 2·BF_4. The comparable stabilities of *i*-Cu^I and *o*-Cu^I were, at least in part, due to the tetrahedral geometry favored by the copper(I) state; therefore, steric repulsion between the methyl group and the auxiliary ligand moieties was not significant in either isomer. The small difference in the *i*-Cu^I ratios of 2·BF_4 and 1·BF_4 was due to the above-mentioned effects of methyl substitution. The isomer ratios are sufficiently valid for use with the simulated fits of the experimental cyclic voltammograms.

The broadening of the ^1H NMR signals recorded under similar conditions indicates that the rate of the rotational interconversion between the *i*-Cu^I and *o*-Cu^I isomers of 1·BF_4 was considerably slower than that of 2·BF_4. The introduction of the methyl group into the 6′-position of the pyridine unit facilitated rotation due to the combined effects of the altered

dx.doi.org/10.1021/ic4011295 | *Inorg. Chem.* 2013, 52, 8962−8970

Table 2. Summary of Rotational Dynamics and Electrochemical Properties of 1·BF_4, 2·BF_4, 3·BF_4, 4·BF_4, and 5·BF_4

		Initial State (Cu^I)		Redox Potential ($Cu^{II/I}$)		Oxidized State (Cu^{II})	
	source	K_I[a]	$k_{Ii\rightarrow o}$[b]	$E^{\circ\prime}{}_o$[c]	$E^{\circ\prime}{}_i$[d]	K_{II}[e]	$k_{IIi\rightarrow o}$[f]
[Cu(Mepypm)(L_{Mes})]BF_4 (1·BF_4)[g]	this work	1.4	2	0.42	0.62	4×10^3	2
[Cu(MepmMepy)(L_{Mes})]BF_4 (2·BF_4)[g]	ref 18f	2.3	20	0.59	0.73	6×10^2	90
[Cu(Mepypm)(DPEphos)]BF_4 (3·BF_4)[h]	ref 18c	2.3	20	[i]	[i]	[i]	[i]
[Cu(Mepypm)(L_{Anth})]BF_4 (4·BF_4)[g]	ref 18a	0.61	1	0.38	0.55	3×10^2	0.3
[Cu(Mepypm)(L_{Macro})]BF_4 (5·BF_4)[g]	ref 18a	0.18	150	0.31	0.46	9×10	15

[a]Equilibrium constant, set as [*o*-Cu^I]/[*i*-Cu^I], at 293 K, estimated from van't Hoff plots. [b]Rate constant for the *i*-$Cu^I \rightarrow$ *o*-Cu^I/s^{-1} at 293 K, estimated from Arrhenius plots. [c]Redox potential for *o*-$Cu^{II/I}$/V vs Ag^+/Ag at 285 K (for 2·BF_4 and 1·BF_4) or 293 K (for 4·BF_4 and 5·BF_4). [d]Redox potential for *i*-$Cu^{II/I}$/V vs Ag^+/Ag. [e]Equilibrium constant, set as [*o*-Cu^{II}]/[*i*-Cu^{II}], at 293 K, estimated from van't Hoff plots. [f]Rate constant for the *i*-$Cu^{II} \rightarrow$ *o*-Cu^{II}/s^{-1} at 293 K, estimated from Arrhenius plots. [g]Based on simulated fits for experimental cyclic voltammograms in Bu_4NBF_4–CH_2Cl_2, considering ^{1}H NMR in CD_2Cl_2. [h]Based on ^{1}H NMR in CD_2Cl_2. [i]Irreversible anodic wave was observed in Bu_4NBF_4–CH_2Cl_2 at room temperature (see Supporting Information, Figure S5).

steric and electronic environments. The increased steric repulsion between the ligand moieties affected by the additional methyl group possibly destabilized the ground state and thereby reduced the energy difference between the ground and the transient states. The energy difference may also have been reduced by the stabilization of the transient state due to the induction effects of the electron-donating methyl group. The rate constants for the *i*-$Cu^I \rightarrow$ *o*-Cu^I rotation of 1·BF_4 ($k_{Ii\rightarrow o}$ = 1 s^{-1} at 285 K, 10^{-5} s^{-1} at 203 K), estimated from the simulated fits of the cyclic voltammograms in Bu_4NBF_4–CH_2Cl_2, were smaller than those of 2·BF_4 ($k_{Ii\rightarrow o}$ = 10 s^{-1} at 285 K, 10^{-4} s^{-1} at 203 K) under similar conditions—this finding is consistent with the sharper ^{1}H NMR signals of 1·BF_4.

The redox potential, $E^{\circ\prime}$, (vs $DMFc^{+/0}$) of *o*-$Cu^{II/I}$ of 2·BF_4 (0.93 V) is similar to that of *i*-$Cu^{II/I}$ of 1·BF_4 (0.99 V), both of which are more positive than that of *o*-$Cu^{II/I}$ of 1·BF_4 (0.79 V) and more negative than that of *i*-$Cu^{II/I}$ of 2·BF_4 (1.07 V). The redox potentials are correlated with the number of the methyl groups around the Cu coordination sphere: 0 for the *o*-isomer of 1·BF_4, 1 for the *o*-isomer of 2·BF_4 and the *i*-isomer of 1·BF_4, and 2 for the *i*-isomer of 2·BF_4. The positive shift of the redox potential is attributed to the steric effects of the methyl substitution, because the destabilization of the copper(II) species makes copper(II)/(I) oxidation thermodynamically less favorable. Methyl substitution did not alter the stability of the tetrahedral geometry favored by the copper(I) species, but it did significantly destabilize the square planar or the 5- or 6-coordinated forms favored by the copper(II) species, because of the steric repulsion between the methyl group and the auxiliary ligand moieties. These results are consistent with the relationships observed between the structure and redox potentials of a family of copper complexes bearing diimines.[12]

The relative stability of *o*-Cu^{II} under equilibrium in the oxidized state was much higher than that of *i*-Cu^{II} in both 2·BF_4 (*i*-Cu^{II}:*o*-Cu^{II} = $1:7 \times 10^2$) and 1·BF_4 (*i*-Cu^{II}:*o*-Cu^{II} = $1:4 \times 10^3$). This was attributed to the *i*-Cu^{II} being more greatly destabilized than *o*-Cu^{II} in the square planar or the 5- or 6-coordinated geometries favored in the copper(II) state, because of steric repulsion between the methyl group and the auxiliary ligand moieties. The causes of these results are essentially similar to those described above, because the redox potentials are related to relative stability and can be used to estimate it.[12]

The rate constants for the *i*-$Cu^{II} \rightarrow$ *o*-Cu^{II} rotation of 1·BF_4 ($k_{IIi\rightarrow o}$ = 2 s^{-1} at 285 K, 10^{-3} s^{-1} at 203 K), estimated from the simulated fits of the cyclic voltammograms in Bu_4NBF_4–CH_2Cl_2, are smaller than those estimated for the equivalent rotation of 2·BF_4 ($k_{IIi\rightarrow o}$ = 50 s^{-1} at 285 K, 10^{-1} s^{-1} at 203 K) under similar conditions. The steric and electronic effects of methyl substitution, which are discussed above, likely contributed to the slower rate of rotation shown by 1·BF_4, compared to 2·BF_4. Steric factors appeared to affect the *i*-$Cu^{II} \rightarrow$ *o*-Cu^{II} rotation more than the *i*-$Cu^I \rightarrow$ *o*-Cu^I rotation, because the greater steric repulsion in *i*-Cu^{II} led to greater destabilization.

Effects of Auxiliary Ligand on Redox Properties and Rotational Dynamics. The effects of the auxiliary ligand were examined through a comparison of 1·BF_4 with other previously reported complexes:[17] [Cu(Mepypm)(DPEphos)]BF_4 (3·BF_4), [Cu(Mepypm)(L_{Anth})]BF_4 (4·BF_4), and [Cu(Mepypm)-(L_{Macro})]BF_4 (5·BF_4), which respectively contain DPEphos, L_{Anth}, and L_{Macro} in place of L_{Mes} (Table 2). The data of 1·BF_4 are described above, and those of 3·BF_4,[17,18c,g] 4·BF_4,[17,18a] and 5·BF_4[17,18a] are reported in our previous works. The auxiliary ligand affected the complexes' rotation and redox behaviors via several factors, such as electronic factors induced by the ligating atom and induction effects, steric repulsion between Mepypm and the auxiliary ligand moieties, and weak interactions.

The *i*-Cu^I ratio of 1·BF_4 (*i*-Cu^I:*o*-Cu^I = 1:1.4), estimated from ^{1}H NMR in CD_2Cl_2 at 293 K, was found to be higher than that of 3·BF_4 (*i*-Cu^I:*o*-Cu^I = 1:2.3). This was at least in part because the *i*-Cu^I isomer of 1·BF_4 was less destabilized than that of 3·BF_4, because of steric repulsion between the methyl group and the auxiliary ligand moieties. Steric repulsion in the *i*-Cu^I isomer of 1·BF_4 appeared to be greater than that in the corresponding *i*-Cu^I isomers of either 4·BF_4 or 5·BF_4. This agrees with the observation of 1·BF_4 showing a lower *i*-Cu^I ratio, as estimated from simulated fits of cyclic voltammograms, than either 4·BF_4 (*i*-Cu^I:*o*-Cu^I = ca. 1:0.6) or 5·BF_4 (*i*-Cu^I:*o*-Cu^I = ca. 1:0.2).

Comparison of the broadening of ^{1}H NMR signals recorded under similar conditions indicates that 1·BF_4 showed a slower rate of rotational interconversion between its *i*-Cu^I and *o*-Cu^I isomers than 3·BF_4 or 5·BF_4. The comparably sharp ^{1}H NMR signals shown by 1·BF_4 and 4·BF_4 indicate their similarly slow rates of rotational interconversion: 1·BF_4 showed a value of $k_{Ii\rightarrow o}$ at 293 K of 2 s^{-1}, estimated from Arrhenius plots based on simulated cyclic voltammograms, which is similar to the 1 s^{-1} reported for 4·BF_4 and much smaller than the 148 s^{-1} reported for 5·BF_4. These results show that the L_{Anth} or L_{Mes} ligands lowered the rate of the interconversion through their bulky groups' occupation of the rotation trajectory, which inhibited rotation kinetically.

Cyclic voltammograms of 1·BF_4, 4·BF_4, and 5·BF_4 in Bu_4NBF_4–CH_2Cl_2 show reversible redox waves derived from

dx.doi.org/10.1021/ic4011295 | Inorg. Chem. 2013, 52, 8962–8970

both *i*-$Cu^{II/I}$ and *o*-$Cu^{II/I}$, and differences in redox potentials between the two rotational isomers of ca. 0.15 V in each case. The redox potential shift is generally due to the destabilization of the *i*-Cu^{II} isomer, as discussed above. The cyclic voltammograms of **3**·BF_4 show irreversible waves at ~0.9 V vs Ag^+/Ag (see Supporting Information, Figure S5), similar to that previously reported for [Cu(Mepypm)(dppp)]BF_4;[18g] the electrochemical properties of **3**·BF_4, whose rotational dynamics and photochemical properties have been previously reported, are reported for the first time here. This irreversibility seems to be caused by an instability of the oxidized [Cu(Mepypm)(diphosphine)]$^+$, which can undergo rapid adverse chemical reactions. Redox irreversibility has also been observed in some [Cu(diimine)(diphosphine)]$^+$ complexes.

The *o*-Cu^{II} isomers were generally more stable than the corresponding *i*-Cu^{II} isomers in **1**·BF_4, **4**·BF_4, and **5**·BF_4, because of the already-discussed destabilization of the *i*-Cu^{II} isomer.

Both **4**·BF_4 and **5**·BF_4 showed lower values of $k_{IIi\rightarrow o}$, estimated from simulated fits of cyclic voltammograms, than the corresponding values of $k_{Ii\rightarrow o}$, because of greater electrostatic interaction in the copper(II) states than in the copper(I) state. In contrast, **1**·BF_4 showed greater values of $k_{IIi\rightarrow o}$ than those of $k_{Ii\rightarrow o}$, because of the electronic and steric effects of the L_{Mes} ligand. A possible contributing factor is the greater steric repulsion between the Mepypm and L_{Mes} moieties in the copper(II) state than in the copper(I) state.

These comparisons demonstrate that both electrochemical properties and rotational dynamics can be finely controlled through the choice of auxiliary ligand. This could be used to tune the functionality of molecular switching systems based on similar complexes.

Photochemistry of 1·BF_4. The absorption spectrum of **1**·BF_4 in CH_2Cl_2 at room temperature is shown in Figure 7a.

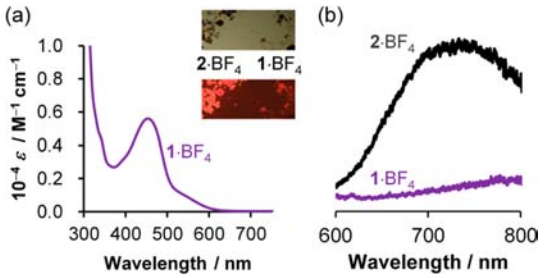

Figure 7. (a) UV–vis absorption spectrum of **1**·BF_4 in CH_2Cl_2 at room temperature. (b) Emission spectra of **1**·BF_4 (purple line) and **2**·BF_4 (black line)[18f] in CH_2Cl_2 at room temperature. Inset: Fluorescence microscopy images of solids of **2**·BF_4 (left) and **1**·BF_4 (right), in bright field (top) and under green-light excitation (bottom) at room temperature.

The absorption band in the visible region (λ_{max} = 454 nm, ε = 5.6 × 10^3 M^{-1} cm^{-1}) was attributed to transitions from the ground state to the singlet MLCT excited state, which is a general property of the bis(diimine)copper(I) complex family.[11,14] The absorption spectrum is similar to that of **2**·BF_4 under similar conditions.[18f] The *i*-Cu^I and *o*-Cu^I isomers of **2**·BF_4 have shown negligible difference in absorption;[18f] therefore, the similar observations of **1**·BF_4 are to be expected. While **2**·BF_4 in CH_2Cl_2 showed a broad emission band in the red region at room temperature,[18f] **1**·BF_4 did not show a corresponding emission band under similar conditions, despite the negligible difference in the optical densities of the two solutions at the light-excitation wavelength (Figure 7b). The greater luminescence of **2**·BF_4 compared with **1**·BF_4 was attributed to the additional methyl group around the copper coordination sphere. This enhancement can be explained via the following effects of substitution on the photochemical properties of a family of copper(I) complexes.[14] First, the inhibition of structural rearrangement contributes to a large energy difference between the ground and photoexcited states; therefore, the nonradiative decay constant is small, because of the energy gap law. Second, additional solvent coordination, which affords nonluminescing 5-coordinated photoexcited species, can be effectively prevented by a crowded coordinated structure. Luminescence microscopy images in the solid state indicate that **2**·BF_4 shows stronger emission than **1**·BF_4 (see Figure 7b).

Effects of Substitution on Photodriven Rotation from a Comparison of 2·BF_4 and 1·BF_4. We have previously reported the mechanism of the photodriven rotation, *i*-Cu^I → *o*-Cu^I, of **2**·BF_4 at 203 K in Bu_4NBF_4–CH_2Cl_2 in the presence of redox mediator, $DMFcBF_4$, to be as follows:[18f]

$$i\text{-}Cu^I + h\nu \rightarrow i\text{-}Cu^I* \quad (1)$$

$$i\text{-}Cu^I* + DMFc^+ \rightarrow i\text{-}Cu^{II} + DMFc^0 \quad (2)$$

$$i\text{-}Cu^{II} \rightarrow o\text{-}Cu^{II} \quad (3)$$

$$o\text{-}Cu^{II} + DMFc^0 \rightarrow o\text{-}Cu^I + DMFc^+ \quad (4)$$

This scheme of four reactions describes: (1) the photoexcitation of a copper(I) complex; (2) photoinduced electron trasnsfer from the photoexcited copper(I) complex to the redox mediator ($DMFc^+$) to produce a transient copper(II) complex and a monoreduced redox mediator, decamethylferrocene ($DMFc^0$); (3) *i*→*o* rotational isomerization at the transient copper(II) state; and (4) a reduction of the copper(II) complex by $DMFc^0$. A metastable copper(I) state can be thermally captured out of the *i*-Cu^I/*o*-Cu^I equilibrium at 203 K by photodriven rotation, *i*-Cu^I → *o*-Cu^I. The inverse of $k_{Ii\rightarrow o}$ ($k_{Ii\rightarrow o}{}^{-1}$) reflects the duration of the entrapment in this metastable state. For example, at 203 K, it is 10^4 s for **2**·BF_4, and for that period, the heat-driven rotation, *o*-Cu^I → *i*-Cu^I, is frozen. The longer value shown by **1**·BF_4 (10^5 s) should contribute to more-efficient photodriven rotation, *i*-Cu^I → *o*-Cu^I, because it represents a slower rate of opposing heat-driven rotation, *o*-Cu^I → *i*-Cu^I.

Cyclic voltammograms of **1**·BF_4 recorded at 203 K in CH_2Cl_2–Bu_4NBF_4 in the presence of 4 equiv $DMFcBF_4$ are displayed in Figure 8a. The two anodic waves for *o*-$Cu^{II/I}$ and *i*-$Cu^{II/I}$ qualitatively reflect the isomer molar ratio of *i*-Cu^I:*o*-Cu^I, which is ca. 1:1 in the initial state. The shape of the voltammograms remained constant in darkness, demonstrating that there were no ongoing processes in the absence of photoirradiation. Irradiation of the solution for 60 min with visible light (λ > 400 nm) induced negligible changes in the voltammograms (Figure 8a). In contrast, the photoirradiation of **2**·BF_4 under similar conditions induced significant convergence of the redox waves to a wave corresponding to *o*-$Cu^{II/I}$ due to photodriven rotation, *i*-Cu^I → *o*-Cu^I.[18f] These results suggest that **2**·BF_4 has a greater ability to undergo photodriven rotation than **1**·BF_4. The irradiation with visible light of **1**·BF_4 at 225 K also caused negligible changes in the voltammograms. The slower heat-driven rotation, *o*-Cu^I → *i*-Cu^I, shown by **1**·BF_4 in comparison with **2**·BF_4 was expected to

dx.doi.org/10.1021/ic4011295 | Inorg. Chem. 2013, 52, 8962–8970

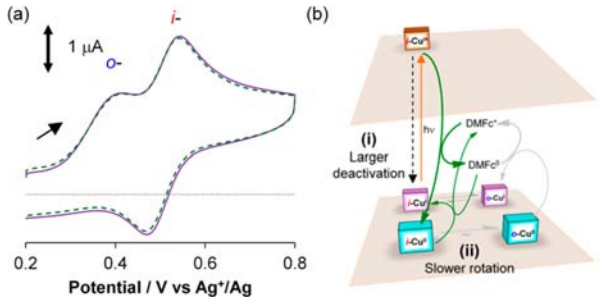

Figure 8. (a) Experimental cyclic voltammograms at a scan rate of 50 mV s^{-1} in the $DMFc^+$ system. The $DMFc^+$ systems comprised **1**·BF_4 in Bu_4NBF_4–CH_2Cl_2 containing 4 equiv $DMFcBF_4$ in darkness at 203 K. Purple line represents the initial state, while the green dotted line represents data after 60 min of visible-light irradiation (λ > 400 nm) at 203 K. (b) The different mechanisms of PET-driven *i*-Cu^I→*o*-Cu^I rotational isomerization in **2**·BF_4[18f] and **1**·BF_4 (this work), in the presence of $DMFc^+$.

give it more-efficient photodriven rotation, *i*-Cu^I → *o*-Cu^I. However, the experimental results showed the opposite, indicating that other factors affected the photodriven rotation more greatly. Inhibited photoinduced electron trasnsfer and slower rotation in the transient copper(II) state are possible causes of the slower photodriven rotation of **1**·BF_4. PET, *i*-Cu^{I*} + $DMFc^+$ → *i*-Cu^{II} + $DMFc^0$, in **1**·BF_4 could be inhibited relative to that in **2**·BF_4, because of the deactivation of the photoexcited state (*i*-Cu^{I*} → *i*-Cu^I + *hν*′ or heat) (Figure 8b). This is because the removal of a methyl group from around the coordination sphere promotes deactivation through the inhibition of both structural rearrangement and solvent coordination quenching in the photoexcited state (the same effects as described in the Photochemistry of **1**·BF_4 section). The slower rotation in the transient copper(II) state, *i*-Cu^{II} → *o*-Cu^{II}, of **1**·BF_4, compared with that of **2**·BF_4, can also aid deactivation, *i*-Cu^{II} + $DMFc^0$ → *i*-Cu^I + $DMFc^+$. These results reveal that methyl substitution on the pyridine moiety is important to the on/off modulation of the photodriven rotation, *i*-Cu^I → *o*-Cu^I.

CONCLUSION

A newly synthesized copper(I) complex, **1**·BF_4, was examined via single-crystal X-ray structural analysis, solution-state NMR measurements, electrochemical measurements, and spectroscopy. Two rotational linkage isomers were shown to coexist (K_I = [*o*-Cu^I]/[*i*-Cu^I] = 1.4 at 293 K) and to interconvert in the solution at room temperature. The difference in the copper(II/I) redox potentials of the two isomers was found to be 0.2 V ($E^{\circ\prime}$ for *i*-$Cu^{II/I}$ = 0.62 V, and $E^{\circ\prime}$ for *o*-$Cu^{II/I}$ = 0.42 V vs Ag^+/Ag at 285 K). Simulated fits of experimental cyclic voltammograms afforded the rate constants of the rotation in the copper(I) ($k_{Ii\rightarrow o}$ = 2 s^{-1} at 293 K) and copper(II) ($k_{IIi\rightarrow o}$ = 2 s^{-1} at 293 K) states. The equilibrium constant of the two isomers in the oxidized state is very large (K_{II} = [*o*-Cu^{II}]/[*i*-Cu^{II}] > 10^3). Increased rotation in the copper(II) state, because of the introduction of a methyl substituent on the pyridine moiety ($k_{IIi\rightarrow o}$ = 90 s^{-1} at 293 K in **2**·BF_4), is important to the photodriven rotation process. These findings are important to the rational molecular design of electric signal switching systems based on single molecular motion.

EXPERIMENTAL SECTION

Materials. **2**·BF_4, **3**·BF_4, and **4**·BF_4 were obtained as described previously. 4-Methyl-2-(2′-pyridyl)pyrimidine (Mepypm),[23] tetrakis(acetonitrile)copper(I) tetrafluoroborate ($[Cu(MeCN)_4]BF_4$),[24] 2,9-dimesityl-1,10-phenanthroline (L_{Mes}),[15] and decamethylferrocenium tetrafluoroborate[25] were also prepared according to methods described in the literature. Other chemicals were used as-received.

Synthesis of [Cu(Mepypm)(L_{Mes})]BF_4 (1·BF_4). Under a nitrogen atmosphere, $[Cu(MeCN)_4]BF_4$ (22 mg, 0.070 mmol) was added to L_{Mes} (30 mg, 0.072 mmol) in 5 mL CH_2Cl_2. To the resultant orange solution, Mepypm (12 mg, 0.072 mmol) was added, and the color of the solution changed immediately to dark red. The reaction mixture was stirred for 30 min and filtered, and diethyl ether (15 mL) was added to precipitate the product, a deep red solid of **1**·BF_4: yield, 27 mg (0.037 mmol, 51%). ^{1}H NMR (500 MHz, CD_2Cl_2, 293 K): δ 8.72 (d, J = 5.0 Hz, *i*-1H), 8.68 (m, *i*-2H + *o*-2H), 8.40 (m, *i*-1H + *o*-1H), 8.20 (s, *i*-2H), 8.18 (s, *o*-2H), 8.11 (m, *i*-1H + *o*-1H), 8.06 (d, *o*-1H), 7.96 (m, *i*-1H + *o*-1H), 7.87 (m, *i*-2H + *o*-2H), 7.45 (m, *o*-1H), 7.24 (d, J = 5.4 Hz, *i*-1H + *o*-1H), 6.35–6.23 (m, *i*-4H + *o*-4H), 2.65 (s, *o*-3H), 2.03 (s, *i*-3H), 1.93 (m, *i*-6H + *o*-6H) 1.76–1.73 (m, *i*-12H + *o*-12H). Elemental analysis. Calculated for $C_{40}H_{37}N_5CuBF_4$: C 65.09, H 5.05, N 9.49. Found: C 64.78, H 5.19, N 9.26.

X-ray Structural Analysis. A red single crystal of **1**·BF_4·1.18CH_2Cl_2 was obtained by diffusing hexane into a dichloromethane solution of **1**·BF_4. Diffraction data were collected with an AFC10 diffractometer coupled with a Rigaku Saturn charge-coupled device (CCD) system equipped with a rotating-anode X-ray generator that produced graphite-monochromated Mo Kα radiation (λ = 0.7107 Å). Lorentz polarization and numerical absorption corrections were performed with the program *Crystal Clear 1.3.6*. The structure was solved by the direct method using *SIR 92* software[26] and refined against F^2 using *SHELXL-97*.[27] *WinGX* software was used to prepare the material for publication.[28] The crystallographic data are listed in Table S1 in the Supporting Information. The isomeric structures were almost identical, except for the position of the methyl group. Occupancy refinement of the crystallographic disorder gave a *i*-:*o*-isomer ratio of 46:54, as analyzed by the *PART* option of the *SHELX-97* program. The disorders of BF_4^- molecules in the crystals were analyzed by the *PART*, *ISOR*, *DELU*, and *SIMU* options of *SHELX-97*.[27] One of the two crystal solvents, CH_2Cl_2, was analyzed by the *DELU* and *ISOR* options of *SHELX-97*.[27]

Instrumentation. NMR spectra at several temperatures were recorded in darkness with a data-recording interval of ca. 20 min, using a Bruker DRX 500 spectrometer. The reported chemical shifts of the solvent residual peaks were used for calibration of the ^{1}H NMR spectra in CD_2Cl_2 (δ 5.32) and acetone-d_6 (δ 2.05).[29] UV–vis absorption spectra were recorded in darkness in quartz cells with an optical path length of 1 cm, using a JASCO Model V-570 spectrometer and a Hewlett-Packard Model 8453 spectrometer equipped with a UNISOKU Model USP-203-A cryostat. Steady-state corrected emission spectra were recorded with a Hitachi Model F-4500 spectrometer. Solid-state luminescence images were measured under green-light excitation using a filter, which is transparent in the red region, and an Olympus BX51 fluorescence microscope. Electrochemical measurements were recorded with an ALS 750A electrochemical analyzer (BAS. Co., Ltd.), equipped with a UNISOKU cryostat. The working electrode was a 0.3 mm O.D. glassy carbon electrode; a platinum wire served as the auxiliary electrode, and the reference electrode was an Ag^+/Ag electrode (a silver wire immersed in 0.1 M Bu_4NClO_4/0.01 M $AgClO_4$/CH_3CN). The solutions were deoxygenated with pure argon prior to the electrochemical measurements. Light irradiation was performed using a MAX-302 xenon lamp (Asahi Spectra) equipped with an optical fiber with a long-pass filter (cut-on 400 nm). Photodriven rotation, *i*-Cu^I → *o*-Cu^I, in the redox mediator system was monitored according to a slight modification of a previously described method.[18f]

Thermodynamic and Kinetic Analysis. The values of K_I = [*o*-Cu^I]/[*i*-Cu^I] of **1**·BF_4 in solution at several temperatures were determined by integration of the ^{1}H NMR signals of the methyl group

dx.doi.org/10.1021/ic4011295 | *Inorg. Chem.* 2013, 52, 8962–8970

on the basis of the pyrimidine moieties. The experimental cyclic voltammograms were simulated using BASi Digisim 3.03a software, based on two independent double-step electron transfer systems. The values of K_{II} = [*o*-Cu^{II}]/[*i*-Cu^{II}] were derived from the experimentally obtained values of K_I and the two redox potentials of *i*-Cu^{II}/*i*-Cu^{I} ($E^{\circ\prime}_i$) and *o*-Cu^{II}/*o*-Cu^{I} ($E^{\circ\prime}_o$). The molar ratios of isomers at various temperatures were calculated from extrapolations of the van't Hoff plots. The rotational rate constants for *i*-Cu^{I} → *o*-Cu^{I} ($k_{Ii\rightarrow o}$), *o*-Cu^{I} → *i*-Cu^{I} ($k_{Io\rightarrow i} = K_I^{-1}k_{Ii\rightarrow o}$), *i*-$Cu^{II}$ → *o*-Cu^{II} ($k_{IIi\rightarrow o}$), and *o*-Cu^{II} → *i*-Cu^{II} ($k_{IIo\rightarrow i} = K_{II}^{-1}k_{IIi\rightarrow o}$) were determined from simulation analysis of the cyclic voltammograms. The rates of rotation at various temperatures were calculated from the slopes and intercepts of the Arrhenius plots. The good fit of the simulated curves with the experimental voltammograms confirmed the validity of the analyses.

■ ASSOCIATED CONTENT

Ⓢ Supporting Information

Crystal structure data (CIF, CCDC No. 936824) and spectral data. Crystallographic data can be obtained free of charge from The Cambridge Crystallographic Data Centre via www.ccdc.cam.ac.uk/data_request/cif. This material is available free of charge via the Internet at http://pubs.acs.org.

■ AUTHOR INFORMATION

Corresponding Author

*E-mail: kume@chem.s.u-tokyo.ac.jp (S.K.), nisihara@chem.s.u-tokyo.ac.jp (H.N.).

Present Addresses

[†]Department of Materials and Life Science, Faculty of Science and Technology, Seikei University, 3-3-1, Kichijoji-kitamachi, Musashino, Tokyo, 180−8633, Japan.

[‡]Department of Chemistry, Graduate School of Science, Hiroshima University, 1-3-1, Kagamiyama, Higashi-Hiroshima, 739−8526, Japan.

Notes

The authors declare no competing financial interest.

■ ACKNOWLEDGMENTS

This work was supported by Grants-in-Aid from MEXT of Japan (Nos. 20750044, 20245013, and 21108002, area 2107 (Coordination Programming)), JST (Research Seeds Quest Program), a Research Fellowship of the Japan Society for the Promotion of Science for Young Scientists, and the Global COE Program for Chemistry Innovation.

■ REFERENCES

(1) (a) O'Regan, B.; Grätzel, M. *Nature* **1991**, *353*, 737−740. (b) Hagfeldt, A.; Grätzel, M. *Acc. Chem. Res.* **2000**, *33*, 269−277. (c) Baldo, M. A.; O'Brien, D. F.; You, Y.; Shoustikov, A.; Sibley, S.; Thompson, M. E.; Forrest, S. R. *Nature* **1998**, *395*, 151−154. (d) Baldo, M. A.; Thompson, M. E.; Forrest, S. R. *Nature* **2000**, *403*, 750−753. (e) Meyer, T. J. *Acc. Chem. Res.* **1989**, *22*, 163−170. (f) Imahori, H.; Tamaki, K.; Guldi, D. M.; Luo, C.; Fujitsuka, M.; Ito, O.; Sakata, Y.; Fukuzumi, S. *J. Am. Chem. Soc.* **2001**, *123*, 2607−2617. (g) Campagna, S.; Puntoriero, F.; Nastasi, F.; Bergamini, G.; Balzani, V. *Top. Curr. Chem.* **2007**, *280*, 117−214. (h) Juris, A.; Balzani, V.; Barigelletti, F.; Campagna, S.; Belser, P.; von Zelewsky, A. *Coord. Chem. Rev.* **1988**, *84*, 85−277.

(2) (a) Park, J.; Pasupathy, A. N.; Goldsmith, J. I.; Chang, C.; Yaish, Y.; Petta, J. R.; Rinkoski, M.; Sthena, J. P.; Abruña, H. D.; McEuen, P. L.; Ralph, D. C. *Nature* **2002**, *417*, 722−725. (b) Joachim, C.; Gimzewski, J. K.; Aviram, A. *Nature* **2000**, *408*, 541−548. (c) Parks, J. J.; aChampagne, A. R.; Costi, T. A.; Shum, W. W.; Pasupathy, A. N.; Neuscamman, E.; Flores-Torres, S.; Cornaglia, P. S.; Aligia, A. A.; Balseiro, C. A.; Chan, G. K. L.; Abruña, H. D.; Ralph, D. C. *Science* **2010**, *328*, 1370−1373.

(3) (a) Sakamoto, R.; Katagiri, S.; Maeda, H.; Nishihara, H. *Coord. Chem. Rev.* **2013**, *257*, 1493−1506. (b) Maeda, H.; Sakamoto, R.; Nishimori, Y.; Sendo, J.; Toshimitsu, F.; Yamanoi, Y.; Nishihara, H. *Chem. Commun.* **2011**, *47*, 8644−8646. (c) Kurita, T.; Nishimori, Y.; Toishimitsu, F.; Muratsugu, S.; Kume, S.; Nishihara, H. *J. Am. Chem. Soc.* **2010**, *132*, 4524−4525. (d) Nishimori, Y.; Kanaizuka, K.; Kurita, T.; Nagatsu, T.; Segawa, Y.; Toshimitsu, F.; Muratsugu, S.; Utsuno, M.; Kume, S.; Murata, M.; Nishihara, H. *Chem.−Asian J.* **2009**, *4*, 1361−1367. (e) Kanaizuka, K.; Murata, M.; Nishimori, Y.; Mori, I.; Nishio, K.; Masuda, H.; Nishihara, H. *Chem. Lett.* **2005**, *34*, 534−535.

(4) (a) Balzani, V.; Credi, A.; Venturi, M. *Molecular Devices and Machines*, 2nd ed.; Wiley−VCH: Weinheim, Germany, 2008. (b) Kay, E. R.; Leigh, D. A.; Zerbetto, F. *Angew. Chem., Int. Ed.* **2007**, *46*, 72−191. (c) Mobian, P.; Kern, J.-M.; Sauvage, J.-P. *Angew. Chem., Int. Ed.* **2004**, *43*, 2392−2395.

(5) (a) Armaroli, N.; Balzani, V.; Collin, J.-P.; Gavina, P.; Sauvage, J.-P.; Ventura, B. *J. Am. Chem. Soc.* **1999**, *121*, 4397−4408. (b) Poleschak, I.; Kern, J. M.; Sauvage, J.-P. *Chem. Commun.* **2004**, 474−476. (c) Collin, J.-P.; Dietrich-Buchecker, C.; Gaviña, P.; Jiménez-Molero, M. C.; Sauvage, J.-P. *Acc. Chem. Res.* **2001**, *34*, 477−487. (d) Sauvage, J.-P. *Acc. Chem. Res.* **1998**, *31*, 611−619. (e) Livoreil, A.; Sauvage, J.-P.; Armaroli, N.; Balzani, V.; Flamigni, L.; Ventura, B. *J. Am. Chem. Soc.* **1997**, *119*, 12114−12124. (f) Sauvage, J.-P. *Bull. Jpn. Soc. Coord. Chem.* **2010**, *55*, 3−18. (g) Livoreil, A.; Dietrich-Buchecker, C. O.; Sauvage, J.-P. *J. Am. Chem. Soc.* **1994**, *116*, 9399−9400. (h) Zahn, S.; Canary, J. W. *J. Am. Chem. Soc.* **2002**, *124*, 9204−9211. (i) Mortezaei, S.; Catarineu, N. R.; Canary, J. W. *J. Am. Chem. Soc.* **2012**, *134*, 8054−8057.

(6) (a) Kume, S.; Nishihara, H. *Dalton Trans.* **2008**, 3260−3271. (b) Nishihara, H. *Coord. Chem. Rev.* **2005**, *249*, 1468−1475. (c) Nishihara, H. *Bull. Chem. Soc. Jpn.* **2004**, *77*, 407−428. (d) Kurihara, M.; Hirooka, A.; Kume, S.; Sugimoto, M.; Nishihara, H. *J. Am. Chem. Soc.* **2002**, *124*, 8800−8801. (e) Namiki, K.; Murata, M.; Kume, S.; Nishihara, H. *New J. Chem.* **2011**, *35*, 2146−2152. (f) Namiki, K.; Sakamoto, A.; Murata, M.; Kume, S.; Nishihara, H. *Chem. Commun.* **2007**, 4650−4652.

(7) (a) Muratsugu, S.; Kume, S.; Nishihara, H. *J. Am. Chem. Soc.* **2008**, *130*, 7204−7205. (b) Sakamoto, R.; Murata, M.; Nishihara, H. *Angew. Chem., Int. Ed.* **2006**, *45*, 4793−4795. (c) Hasegawa, Y.; Takahashi, K.; Kume, S.; Nishihara, H. *Chem. Commun.* **2011**, *47*, 6846−6848. (d) Takahashi, K.; Hasegawa, Y.; Sakamoto, R.; Nishikawa, M.; Kume, S.; Nishibori, E.; Nishihara, H. *Inorg. Chem.* **2012**, *51*, 5188−5198. (e) Umeki, S.; Kume, S.; Nishihara, H. *Inorg. Chem.* **2011**, *50*, 4925−4933. (f) Nagashima, S.; Murata, M.; Nishihara, H. *Angew. Chem., Int. Ed.* **2006**, *45*, 4298−4301.

(8) (a) Kume, S.; Murata, M.; Ozeki, T.; Nishihara, H. *J. Am. Chem. Soc.* **2005**, *127*, 490−491. (b) Umeki, S.; Kume, S.; Nishihara, H. *Chem. Lett.* **2010**, *39*, 204−205. (c) Kume, S.; Kurihara, M.; Nishihara, H. *Inorg. Chem.* **2003**, *42*, 2194−2196.

(9) (a) Fraysse, S.; Coudret, C.; Launay, J.-P. *Eur. J. Inorg. Chem.* **2000**, 1581−1590. (b) Tanaka, Y.; Inagaki, A.; Akita, M. *Chem. Commun.* **2007**, 1169−1171.

(10) (a) Irie, M. *Chem. Rev.* **2000**, *100*, 1685−1716. (b) Irie, M.; Fukaminato, T.; Sasaki, T.; Tamai, N.; Kawai, T. *Nature* **2002**, *420*, 759−760. (c) Kobatake, S.; Takami, S.; Muto, H.; Ishikawa, T.; Irie, M. *Nature* **2007**, *446*, 778−781. (d) Gorostiza, P.; Isacoff, E. Y. *Science* **2008**, *322*, 395−399. (e) Durr, H. *Photochromism: Molecules and Systems*; Elsevier: Amsterdam, 1990. (f) Uchida, K.; Yamanoi, Y.; Yonezawa, T.; Nishihara, H. *J. Am. Chem. Soc.* **2011**, *133*, 9239−9241.

(11) (a) Ruthkosky, M.; Kelly, C. A.; Castellano, F. N.; Meyer, G. J. *Coord. Chem. Rev.* **1998**, *171*, 309−322. (b) Scaltrito, D. V.; Thompson, D. W.; O'Callaghan, J. A.; Meyer, G. J. *Coord. Chem. Rev.* **2000**, *208*, 243−266. (c) Ruthkosky, M.; Castellano, F. N.; Meyer, G. J. *Inorg. Chem.* **1996**, *35*, 6406−6412.

(12) (a) Miller, M. T.; Gantzel, P. K.; Karpishin, T. B. *Inorg. Chem.* **1998**, *37*, 2285−2290. (b) Rorabacher, D. B. *Chem. Rev.* **2004**, *104*, 651−697. (c) Le Poul, N.; Campion, M.; Douziech, B.; Rondelez, Y.;

Le Clainche, L.; Reinaud, O.; Le Mest, Y. *J. Am. Chem. Soc.* **2007**, *129*, 8801−8810. (d) Meyer, M.; Albrecht-Gary, A. M.; Dietrich-Buchecker, C. O.; Sauvage, J.-P. *Inorg. Chem.* **1999**, *38*, 2279−2287. (e) Munakata, M.; Endicott, J. F. *Inorg. Chem.* **1984**, *23*, 3693−3698. (f) Munakata, M.; Kitagawa, S.; Asahara, A.; Masuda, H. *Bull. Chem. Soc. Jpn.* **1987**, *60*, 1927−1929. (g) Federlin, P.; Kern, J.-M.; Rastegar, A.; Dietrich-Buchecker, C.; Marnot, P. A.; Sauvage, J.-P. *New. J. Chem.* **1990**, *14*, 9−12.

(13) (a) Lacour, J.; Moraleda, D. *Chem. Commun.* **2009**, 7073−7089. (b) Hebbe-Viton, V.; Desvergnes, V.; Jodry, J. J.; Dietrich-Buchecker, C.; Sauvage, J.-P.; Lacour, J. *Dalton Trans.* **2006**, 2058−2065. (c) Desvergnes-Breuil, V.; Hebbe, V.; Dietrich-Buchecker, C.; Sauvage, J.-P.; Lacour, J. *Inorg. Chem.* **2003**, *42*, 255−257. (d) Hutin, M.; Nitschke, J. R. *Chem. Commun.* **2006**, 1724−1726. (e) Riesgo, E.; Hu, Y.-Z.; Bouvier, F.; Thummel, R. P. *Inorg. Chem.* **2001**, *40*, 2541−2546. (f) Frei, U. M.; Geier, G. *Inorg. Chem.* **1992**, *31*, 187−190.

(14) (a) Armaroli, N.; Accorsi, G.; Cardinali, F.; Listorti, A. *Top. Curr. Chem.* **2007**, *280*, 69−115. (b) Lavie-Cambot, A.; Cantuel, M.; Leydet, Y.; Jonusauskas, G.; Bassani, D. M.; McClenaghan, N. D. *Coord. Chem. Rev.* **2008**, *252*, 2572−2584. (c) McMillin, D. R.; McNett, K. M. *Chem. Rev.* **1998**, *98*, 1201−1219. (d) Barbieri, A.; Accorsi, G.; Armaroli, N. *Chem. Commun.* **2008**, 2185−2193.

(15) (a) Schmittel, M.; Michel, C.; Wiegrefe, A.; Kalsani, V. *Synthesis* **2001**, *10*, 1561−1567. (b) Schmittel, M.; Ganz, A. *Chem. Commun.* **1997**, 999−1000. (c) Schmittel, M.; Michel, C.; Liu, S.-X.; Schildbach, D.; Fenske, D. *Eur. J. Inorg. Chem.* **2001**, 1155−1166. (d) Schmittel, M.; Lüning, U.; Meder, M.; Ganz, A.; Michel, C.; Herderich, M. *Heterocycl. Commun.* **1997**, *3*, 493−498.

(16) (a) Cuttell, D. G.; Kuang, S. M.; Fanwick, P. E.; McMillin, D. R.; Walton, R. A. *J. Am. Chem. Soc.* **2002**, *124*, 6−7. (b) Kuang, S. M.; Cuttell, D. G.; McMillin, D. R.; Fanwick, P. E.; Walton, R. A. *Inorg. Chem.* **2002**, *41*, 3313−3322. (c) Hsu, C.-W.; Lin, C.-C.; Chung, M.-W.; Chi, Y.; Lee, G.-H.; Chou, P.-T.; Chang, C.-H.; Chen, P.-Y. *J. Am. Chem. Soc.* **2011**, *133*, 12085−12099. (d) Smith, C. S.; Branham, C. W.; Marquardt, B. J.; Mann, K. R. *J. Am. Chem. Soc.* **2010**, *132*, 14079−14085. (e) Iwamura, M.; Watanabe, H.; Ishii, K.; Takeuchi, S.; Tahara, T. *J. Am. Chem. Soc.* **2011**, *133*, 7728−7736. (f) Siddique, Z. A.; Yamamoto, Y.; Ohno, T.; Nozaki, K. *Inorg. Chem.* **2003**, *42*, 6366−6378. (g) Saito, K.; Arai, T.; Takahashi, N.; Tsukuda, T.; Tsubomura, T. *Dalton Trans.* **2006**, 4444−4448.

(17) Nishikawa, M.; Kume, S.; Nishihara, H. *Phys. Chem. Chem. Phys.* **2013**, *15*, 10549−10565.

(18) (a) Nomoto, K.; Kume, S.; Nishihara, H. *J. Am. Chem. Soc.* **2009**, *131*, 3830−3831. (b) Kume, S.; Nomoto, K.; Kusamoto, T.; Nishihara, H. *J. Am. Chem. Soc.* **2009**, *131*, 14198−14199. (c) Nishikawa, M.; Nomoto, K.; Kume, S.; Inoue, K.; Sakai, M.; Fujii, M.; Nishihara, H. *J. Am. Chem. Soc.* **2010**, *132*, 9579−9581. (d) Kume, S.; Nishihara, H. *Chem. Commun.* **2011**, *47*, 415−417. (e) Kume, S.; Nishihara, H. *Dalton Trans.* **2011**, *40*, 2299−2305. (f) Nishikawa, M.; Nomoto, K.; Kume, S.; Nishihara, H. *J. Am. Chem. Soc.* **2012**, *134*, 10543−10553. (g) Nishikawa, M.; Nomoto, K.; Kume, S.; Nishihara, H. *Inorg. Chem.* **2013**, *52*, 369−380.

(19) (a) Example for other type of coordinated ligand rotational isomerization such as based on Rh═C double bond. McCormick, F. B.; Kiel, W. A.; Gladysz, J. A. *Organometallics* **1982**, *1*, 405−408. (b) The photocatalyst ability of $[Cu(Mepypm)(DPEphos)]^+$ has been reported. Hernandez-Perez, A. C.; Vlassova, A.; Collins, S. K. *Org. Lett.* **2012**, *14*, 2988−2991.

(20) Electrochemical methods for a square scheme, such as interpretation for convergence of redox waves and simulation of voltammograms, described below, are well-established: (a) Bain, A. D. *Prog. Nucl. Magn. Reson. Spectrosc.* **2003**, *43*, 63−103. (b) Sandström, J. *Dynamic NMR Spectroscopy*; Academic Press: London, 1982.

(21) Hiraoka, S.; Hisanaga, Y.; Shiro, M.; Shionoya, M. *Angew. Chem., Int. Ed.* **2010**, *49*, 1669−1673.

(22) (a) Bard, A. J.; Faulkner, L. R. *Electrochemical Methods, Fundamentals and Applications*, 2nd ed.; Wiley: New York, 2001. (b) Jacq, J. *J. Electroanal. Chem.* **1971**, *29*, 149−180. (c) Carano, M.; Echegoyen, L. *Chem.—Eur. J.* **2003**, *9*, 1974−1981. (d) Lerke, S. A.; Evans, D. H.; Feldberg, S. W. *J. Electroanal. Chem.* **1990**, *296*, 299−315.

(23) Lafferty, J. J.; Case, F. H. *J. Org. Chem.* **1967**, *32*, 1591−1596.

(24) Merrill, C. L.; Wilson, L. J.; Thamann, T. J.; Loehr, T. M.; Ferris, N. S.; Woodruff, W. H. *J. Chem. Soc., Dalton Trans.* **1984**, 2207−2221.

(25) Tabbi, G.; Cassino, C.; Cavigiolio, G.; Colangelo, D.; Ghiglia, A.; Viano, I.; Osella, D. *J. Med. Chem.* **2002**, *45*, 5786−5796.

(26) Altomare, A.; Cascarano, G.; Giacovazzo, C.; Guagliardi, A.; Burla, M. C.; Polidori, G.; Camalli, M. *J. Appl. Crystallogr.* **1994**, *27*, 435.

(27) Sheldrick, G. M. *Acta Crystallogr., Sect. A: Found. Crystallogr.* **2008**, *A64*, 112−122.

(28) Farrugia, L. J. *J. Appl. Crystallogr.* **1999**, *32*, 837−838.

(29) Fulmer, G. R.; Miller, A. J. M.; Sherden, N. H.; Gottlieb, H. E.; Nudelman, A.; Stoltz, B. M.; Bercaw, J. E.; Goldberg, K. I. *Organometallics* **2010**, *29*, 2176−2179.